OUKA
The University of Osaka
Institutional Knowledge Archive

Title	Nanoindentation Hardness Test for Estimation of Vickers Hardness
Author(s)	Kato, Hiroshi; Takahashi, Makoto; Ikeuchi, Kenji
Citation	Transactions of JWRI. 2006, 35(1), p. 57-61
Version Type	VoR
URL	https://doi.org/10.18910/12769
rights	
Note	

The University of Osaka Institutional Knowledge Archive : OUKA

https://ir.library.osaka-u.ac.jp/

The University of Osaka

Nanoindentation Hardness Test for Estimation of Vickers Hardness†

KATO Hiroshi*, TAKAHASHI Makoto, and IKEUCHI Kenji*****

Abstract

The nanoindentation hardness test has been carried out on stainless steel SUS 316 plates cold-worked to various degrees to develop a method for estimating the hardness based on the direct observation of the residual impression in nano-meter scale with an atomic force microscope. A relation between the Vickers hardness and the indentation hardness estimated from the projected area of the residual impression was obtained. The conventional method using the penetration depth h_p of the indenter showed that a similar relation also held between the indentation hardness and the Vickers hardness. The hardness estimated from the penetration depth h_p, however, was much more strongly influenced by the inflatness of the specimen surface than that estimated from projected area of the impression

KEY WORDS: (Nanoindentation hardness), (Vickers hardness), (Stainless steel), (Atomic force microscope), (Berkovich indenter)

1. Introduction

The Vickers hardness is widely employed as a measure or indicator of materials properties and performance. For example, the sensitivity of the steel weld HAZ (Heat Affected Zone) to hydrogen delayed cracking, a major factor controlling the weldability of high strength steel, is a function of the maximum Vickers hardness of the HAZ, which is limited below 300 HV in many cases. It is known that austenitic stainless steels SUS304 and SUS316 become susceptible to stress corrosion cracking in high temperature water, when their hardness exceeds ～300 HV[1)]. The Vickers hardness is also used as an indicator of C content in the martensite[2)].

The application field of the Vickers hardness test, however, has a limit coming from the size of the residual impression. It is known that the distance from an impression to neighboring impressions must be more than 2.5 times as great as the impression sizes in order to avoid the interference from the strain field set up around the neighboring impressions. Since the size of impression from which reliable hardness value can be determined must be not less than 5-10 μm (resolution of the optical microscope ～ 1 μm), the conventional Vickers hardness test is difficult to use for the estimation of the hardness in areas narrower than few 10 μm in size: for example, the work-hardened layer introduced into the metal surface by heavy mechanical grinding and the intermetallic compound layer forming at a joint interface between dissimilar metals. The measurement of hardness of such narrow areas requires the development of a method to determine the hardness from an impression less than 1 μm in size.

Recently, the nanoindentation hardness test has been developed, which enables the estimation of the mechanical properties of thin film and small volumes of materials from a relation between the indentation load and penetration depth of the indenter. In this test, the penetration depth is measured at the nano meter (10^{-9} m) scale instead of determining the residual impression size with a light microscope. The present investigation was aimed at developing a new technique of the nanoindentation hardness test based on the observation of the residual impression with an atomic force microscope to estimate the Vickers hardness in an area at a distance less than few μm from the surface.

2. Experimental Details

The specimen for the hardness test was cut from a

† Received on May 12, 2006
* Graduate Student
** Instructor
*** Professor

Transactions of JWRI is published by Joining and Welding Research Institute, Osaka University, Ibaraki, Osaka 567-0047, Japan

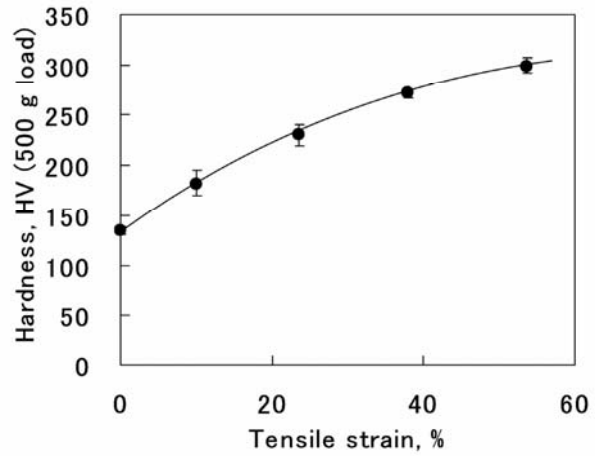

Fig. 1 Relation between the Vickers hardness and tensile strain for a stainless steel SUS316 plate.

plate of a solution-treated austenitic stainless steel SUS316. The Vickers hardness of the specimen was changed from 135 HV to 310 HV by applying tensile strain up to ~55% (nominal strain). The Vickers hardness of the specimen is shown as a function of tensile strain in **Fig. 1**. Specimens having hardness higher than that shown in this figure were obtained by cold-rolling subsequent to the application of a tensile strain of ~55% (fracture strain). The surface of the specimen was finished by grinding on metallographic paper up to 2000 grade, and subsequent electropolishing at 253 K in an ethanol solution containing 8% hydrochloric acid, 12% water, and 10% 2-butoxyethanol by volume. The hardness measurement was carried out with a Shimadzu Nanoscopic Surface Indenter SPH-1. The indenter employed was the Berkovich type with a face angle of 65.3°, which gives the same projected area-to-depth ratio as the Vickers indenter. The indentation cycle consisted of loading, holding at a maximum load, and unloading. The loading and unloading rates were 0.1 mN/s. The maximum load was 1 mN and the holding time was 5 s unless otherwise stated.

3. Experimental Results and Discussion

In the conventional hardness test, the area of contact between the indenter and specimen is calculated directly from the measured dimensions of the residual impression left in the specimen surface after the removal of the indentation load, and the hardness is given by dividing the indentation load by the contact area. Two types of the contact area were employed depending on the kinds of hardness[3]: the whole contact area on the indenter surface and the contact area projected to the basal plane of the indenter. In the nanoindentation hardness test, the projected contact area is indirectly determined from the depth of the penetration of the indenter into the specimen. The penetration depth is estimated from the load-displacement (= penetration depth) curve as shown in **Fig. 2**. These were obtained from nanoindentation

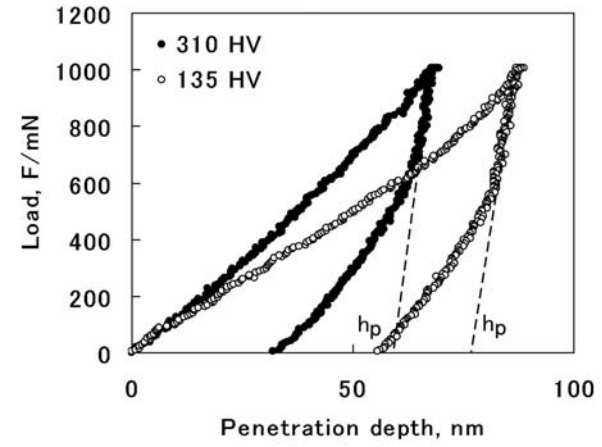

Fig. 2 Load – displacement curves obtained from nanoindentation tests for SUS316 specimens in as-solution-treated state (135 HV) and deformed by 55% (310 HV) in tension.

hardness tests on stainless steel SUS316 specimens having the Vickers hardness of 130HV and 310HV. Usually, the penetration depth h_p, which is obtained from the intercept of the displacement axis (load = 0 mN) with a tangent to the unloading curve at the maximum load, is employed to estimate the projected contact area. From the geometry of the Berkovich indenter having face angle of 65.3°, the projected contact area A_p to support the maximum load F can be given by

$$A_p = 24.49\, h_p^2 .$$

The indentation hardness H_{IT} (kg/mm^2) which is defined as the mean contact pressure beneath the contact area of the indenter is expressed by

$$H_{IT} = F/A_p = F / (24.49\, h_p^2).$$

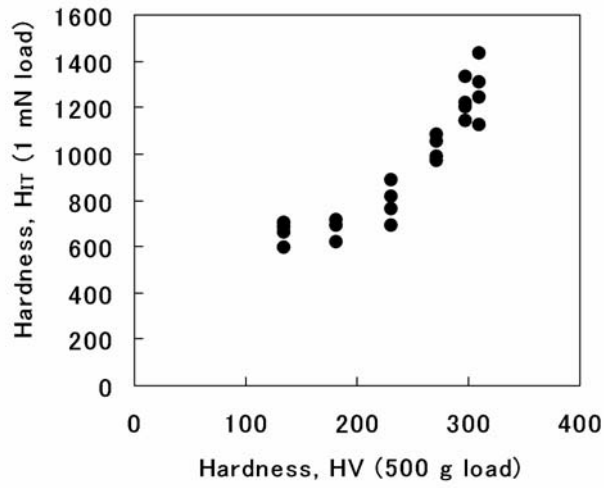

Fig. 3 Indentation hardness H_{IT} estimated from the penetration depth h_p as a function of the Vickers hardness for SUS316 specimens deformed by 0 – 55%.

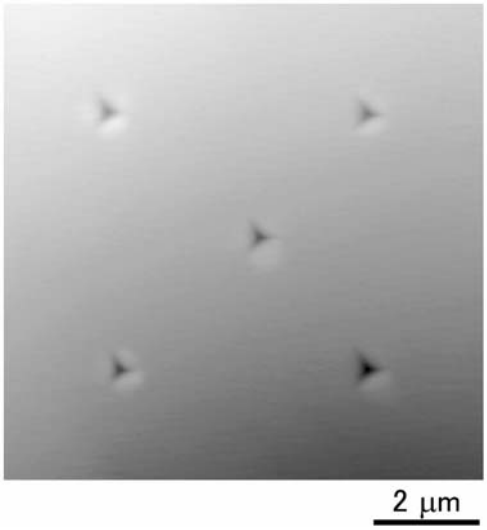

Fig. 4 AFM images of residual impressions formed in a surface of a SUS316 specimen after the nanoindentation test at a maximum load of 1 mN.

The indentation hardness estimated from the penetration depth h_p is plotted against the Vickers hardness in **Fig. 3**. The indentation hardness value estimated from the penetration depth h_p increased with the Vickers hardness, though higher than the Vickers hardness by 4 - 5 times.

On the other hand, the topographic image of the residual impression can be obtained from the observation with an atomic force microscope (which is attached to the instrument used for the nanoindentation test) as shown in **Fig. 4**. This topographic image can be utilized to estimate the projected area of contact. An enlarged image of a residual impression is shown in **Fig. 5(a)**, and its section profile along the line A-B can be obtained as shown in **Fig.5(c)**. The profile of the original surface can be obtained by extrapolating from surfaces profiles of areas far from the impression. From a comparison of the impression profile with the original surface profile, points 'a' and 'b' were taken as the edges of the impression. The edges of the impression on lines C-D and E-F were determined similarly. As shown in **Fig.5 (b)**, sets of three points 'd-a-f', 'f-c-b', and 'b-c-d' lay along almost straight lines, suggesting that these points were determined properly. The projected area S of the impression is given by the following equation

$$S = \{s\,(s\text{-}L_1)\,(s\text{-}L_2)\,(s\text{-}L_3)\}^{1/2},$$

where L_1, L_2, and L_3 are the lengths of the three sides of triangle bdf, and $s = (L_1+L_2+L_3)/2$. In **Fig. 6**, the indentation hardness estimated from the projected area S is plotted against the Vickers hardness. Although the obtained indentation hardness was scattered widely, it tends to increase with the Vickers hardness. The indentation hardness values estimated from the projected contact area S were closer to the Vickers hardness than that estimated from the penetration depth h_p. The hardness value estimated from the projected area increased with the Vickers hardness, showing a general tendency similar to that estimated from the penetration depth h_p. When the indentation load was increased to 2 mN, the estimated hardness was slightly decreased and the scatter range of the hardness was narrowed as shown in Fig.6. As shown in Fig.6, hardness values estimated from the penetration depth h_p and the contact area S were significantly higher than the Vickers hardness. Since the Vickers hardness is calculated from the whole contact area on the indenter surface[4], the Vickers hardness is

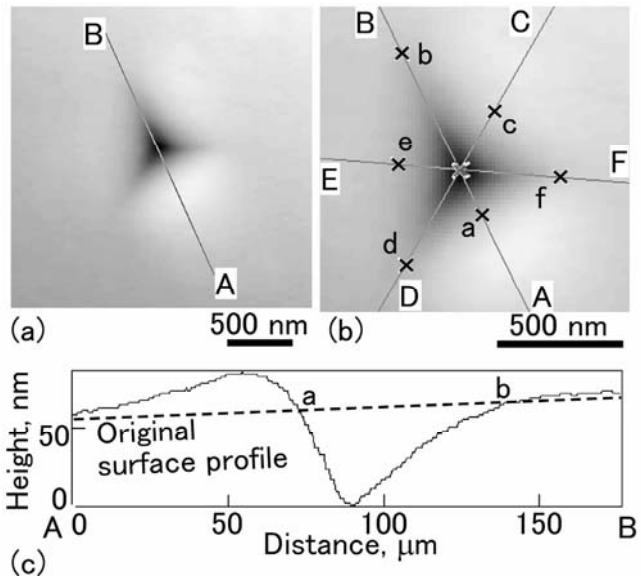

Fig. 5 (a) Enlarged image of a residual impression, (b) edges of the impressions determined from section profiles along lines A-B, C-D and E-F, and (c) section profile of the impression along line A-B.

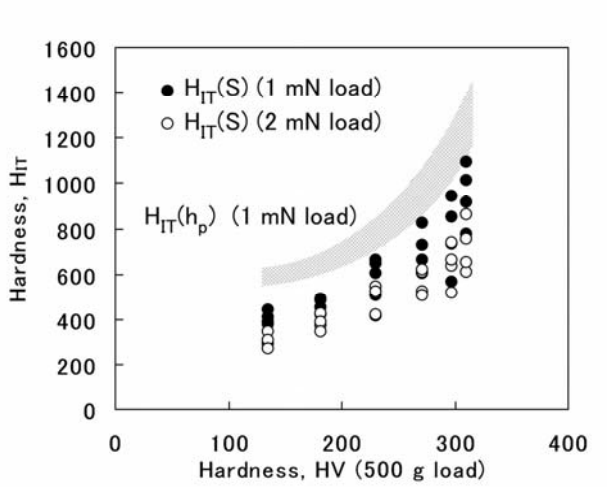

Fig. 6 Indentation hardness H_{IT} estimated from the projected area of the residual impression S as a function of the Vickers hardness for SUS316 specimens, where H_{IT} estimated from the penetration depth h_p is also shown for comparison.

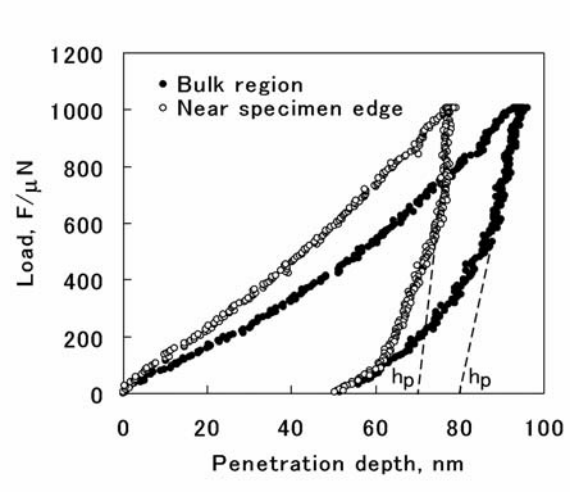

Fig. 7 Load – displacement curves obtained from nanoindentation tests made near the edge of specimen and in the bulk region for a SUS316 specimen.

smaller than the indentation hardness. From the geometry of the Vickers indenter, however, the difference between them is about 7%. (According to ISO standards, the unit of H_{IT} is (N/mm^2), but in this paper H_{IT} is expressed in (kg/ mm^2) unit for the convenience of the comparison with HV (kg/ mm^2)). Thus, the difference between the measured values of the indentation hardness and the Vickers hardness is much greater than the theoretical prediction. With respect to the difference between the Vickers hardness value and the nanoindentation hardness, many authors[5-7] reported that it becomes greater as the penetration depth, i.e., contact area becomes smaller. However, to our knowledge, none of them provided a theoretical basis to explain it. Thus, the indentation hardness estimated from the projected areas of the residual impression and penetration depth h_p (by a conventional method) had relations with the Vickers hardness showing a similar general tendency, although the estimation from the penetration depth h_p yielded slightly higher hardness values than from the contact area S.

The specimen surface for the nanoindentation hardness test is usually finished by electropolishing in order to avoid the influence of work hardening introduced into the surface layer during mechanical grinding and polishing. Since the work hardening has a stronger influence on the estimated hardness value as the penetration depth becomes smaller, the surface finishing by a chemical process like electropolishing is a prerequisite for the hardness measurement of a very narrow area. It should be noted that the rate of electropolishing is significantly enhanced near the edge of a specimen and the interface between dissimilar materials because of the so-called edge effect. This effect impairs the flatness of the surface near edge of the specimen and the interface between dissimilar materials.

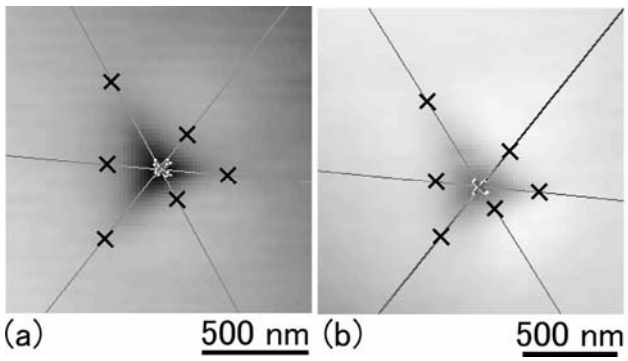

Fig. 8 AFM images of residual impressions and their edges determined from the section profiles: (a) in the bulk region and (b) near the specimen edge.

Therefore, we investigated the effects of the inflatness of the surface near the specimen edge on the hardness measurement based on the penetration depth h_p and the projected area S of the residual impression. A load-displacement curve obtained from the nanoindentation hardness test near the specimen edge is compared with one obtained in the bulk region in **Fig. 7**. The penetration depth observed near the specimen edge was significantly smaller than that observed in the bulk region, and the unloading curve observed near the specimen edge showed incomprehensive flexions. The indentation hardness value estimated from the penetration depth h_p was 910 near the specimen edge, while it was 580 in the bulk region.

On the other hand, AFM images observed near the specimen edge and in the bulk region are shown in **Figs. 8(a)** and **8(b)**, respectively. The hardness values estimated from the projected areas of these impressions were 545 near the specimen edge and 530 in the bulk region, and so they can be considered to be much less influenced by the inflatness of the specimen surface than those estimated from the penetration depth. Thus it can be concluded that the projected area S of the residual impression measured directly from the AFM image is preferable to the penetration depth for the hardness measurement in narrow areas near the specimen edge and dissimilar materials interface.

4. Conclusions

The nanoindentation hardness test has been carried out on stainless steel SUS 316 plates cold-worked to various degrees to develop a method for estimating the hardness based on the direct observation of the residual impression at the nano-meter scales with an atomic force microscope. The results obtained are summarized as follows:

(1) A relation between the Vickers hardness and the indentation hardness estimated from the projected area of the residual impression was obtained. This relation showed a similar general tendency to that between the Vickers hardness and indentation hardness estimated from the penetration depth h_p of the indenter based on the conventional method. The estimation from the projected area of the residual impression yielded hardness values closer to the Vickers hardness.

(2) The hardness estimated from the penetration depth h_p was strongly influenced by the inflatness of the specimen surface, while the projected area of the impression and estimated hardness were almost independent of the inflatness of the surface.
(3) The indentation hardness values estimated from the penetration depth h_p and from the projected area of the impression were much higher than those calculated from the Vickers hardness. Further investigations are in progress to explain this difference.

Acknowledgement

The authors wish to thank Dr. H. Ito with Nuclear Plant Service Engineering Co. Ltd. for his valuable discussion and providing the specimen of the stainless steel used in this investigation.

References

1) Y. Kaneshima, N. Totsuka and K. Arioka: SCC Susceptibility of Plastic Deformed Austenitic Stainless Steel, J. Institute of Nuclear Safety System 2002, 9(2002). pp. 109-115 (in Japanese).
2) G.Krauss: *Steel: Processing, Structure, and Performance*, ASM International, (2005), p. 299.
3) K. Miyahara, N. Nagashima, S. Matsuoka, and T. Ohmura: Evaluation of Vickers Hardness by Nanoindentation Measurement, Trans. Japan Soc. Mech. Eng. A, 64-626(1998), pp. 2567-2573 (in Japanese).
4) A.C. Fischer-Cripps: *Nanoindentation*, Springer, (2004), p. 26.
5) W.C. Oliver and G.M. Pharr: An improved technique for determining hardness and elastic modulus using load and displacement sensing indentation experiments, J. Mater. Res., 7-6(1992), pp. 1564-1583.
6) J.A. Knapp, D.M. Follstaedt, S.M. Myers, J.C.Barbour, and T.A. Friendann: Finite-element modeling of nanoindentation, J. Appl. Phys., 85-3(1999), pp1460-1473.
7) M. Seo, M. Chiba, and Y. Kurata: Nano-indentation to the Passive Metal Surface in Solution, Zairyo-to-Kankyo, 52-1(2002), pp5-11 (in Japanese).